Ring Bank Theory of Conscious Semiosis: Access Geometry, Baseline Dynamics, and Aboutness Modulation

Brad Caldwell, BSCE
caldwbr@gmail.com

April 12, 2026

Abstract

Ring Bank Theory (RBT) is a geometric, access-first account of conscious semiosis. The theory posits a perspective-invariant **Bank** $\mathcal{B}$ (a shape manifold acted on by Sim(3)), a dynamic, low-dimensional **Access Manifold** $\mathcal{A}(t)$ on which conscious sampling/printing occurs, and a **Time Schema** $\mathcal{T}$ that turns discrete prints into apparent flow. **Real** ($\mathcal{R}$) and **Imaginal** ($\mathcal{I}$) schemas are readouts reconstructed with characteristic latency (yet extrapolating predictively into the present) from recent ringframes ρ produced by a **printing operator** Π acting on $\mathcal{A}$. A **hierarchical mapping architecture** anchors all schema poses to the Real Schema Avatar $\mathcal{R}_{\mathrm{A}}$ via a primary mapping $\Phi_{\mathcal{R}_{\mathrm{A}}\to\mathcal{A}}$, with Bank, Real, and Imaginal schemas slaved through secondary couplings. **Baseline dynamics** supply cadence (spirographic, stationary, chirp), while **aboutness modulation** provides context-sensitive adjustments of pose (via Sim(3)), intra-bank walks, and timing. **Pose-jet** control extends modulation beyond instantaneous pose to velocity, acceleration, and higher-order kinematic texture, while **orbital parameter jets** allow the system to modulate how the Bank's orbit itself evolves. A point-process **hazard** $h(t)$ mixes baseline rhythm, high-level "mic" events $\mathcal{M}$, and adaptation to schedule interrupt-like prints, while phasic modes are continuously modulated rather than gated. The framework yields testable predictions for hyperpolarization bottlenecks, photic entrainment, cardiac-phase effects, vestibular "throw," and dual-plane refresh, and it integrates classic phenomenology (rings, bank skewer, vibes, paint) with Lie-group posing and point-process statistics [7–10].

Keywords: consciousness, semiosis, geometry, shape space, similarity group, hybrid dynamical system, hazard function, cross-frequency coupling, retrosplenial cortex, pulvinar, DMN, dissociation.

1 Introduction

RBT treats conscious experience as *semiosis in motion*. Instead of beginning with content, RBT begins with *when and where* access happens, and lets *what* (paint/semantics) be the downstream consequence. We articulate three organizing claims:

1. **Access-first geometry.** Conscious sampling occurs on a transient, low-dimensional *Access Manifold* $\mathcal{A}(t)$ embedded in a posed *Bank* $\mathcal{B}$ (a shape manifold under Sim(3)). A printing operator Π writes ringframes $\rho(t)$ that populate a fading *Time Schema* $\mathcal{T}$.

2. **Baseline vs. aboutness.** A slow *baseline* sets macro-cadence and bank behavior; *aboutness modulation* steers pose, intra-bank walks, and timing so that access meets the currently relevant object of thought or action.

3. **Semiosis as cascade.** A Peircean-style three-stage cascade links mic/baseline driven prints (representamina) to $\mathcal{R}/\mathcal{I}$ readouts (interpretants) and then to threats/affordances and action (objects) [6]. Aboutness is sometimes controlled, often modulated.

A fourth claim, developed in detail below, concerns the *hierarchical mapping architecture* that organizes all schema poses around the Real Schema Avatar $\mathcal{R}_{\mathrm{A}}$, and the *jet-level control* that extends modulation beyond instantaneous pose to velocity, acceleration, and higher-order kinematic texture.

This paper consolidates prior drafts into a self-consistent formalization, gives precise operational definitions for modes of printing, and outlines falsifiable predictions aligned with neural observations in dissociation/hyperpolarization and task-related dynamics [3–5, 7, 8].

2 Core objects

2.1 Bank ($\mathcal{B}$): 3D shape space with $\mathrm{Sim}(3)$ action

In plain terms, the Bank is largely a cube/sphere agglomerated object, with hundreds of concentric copies scaling inwards. In reality, every shape you model stores lightly upon it. Let $\mathcal{S}$ denote a shape space of configurations modulo translation, rotation, and scale (*Kendall-type* shape space). The Bank $\mathcal{B}$ could be thought of as a single, extremely complex shape, and as such, could be considered a latent point (or submanifold) $S \in \mathcal{S}$ encoding perspective-invariant relational geometry (compare Lehar's concentric scaffolds [9, 10]). A conscious *display* chooses a pose $g(t) \in \mathrm{Sim}(3)$ acting on a canonical representative:

$$X_{\mathrm{display}}(t) := g(t) \cdot S, \qquad g(t) = \big(s(t), R(t), t(t)\big), \quad R(t) \in \mathrm{SO}(3) \tag{1}$$

Content and context can restrict $g(t)$ to a *coset* $g(t)H$ where H stabilizes S (symmetries). This separation of *shape* (what) and *pose* (where/how big) makes *attitude misalignment* precise: e.g., a yaw error is a systematic rotation in $R(t)$ between body- and environment-subspaces (cf. grasp underreach anecdote).

2.2 Real schema ($\mathcal{R}$): 3D veridical world model for action

The real schema $\mathcal{R}$ is the 3D understanding of the immediate world that guides the body schema and physical movement. It consists of:

- **Stereo geometry**: Left-eye and right-eye volumes merged into a cyclopean view behind the nose via rotation around the focal object,
- **Hierarchical structure**: Nested schemas including body, environment, and key object representations,
- **Dual temporal modes**: Both static (present snapshot) and dynamic (changing world) representations.

As the servo target for physical action, $\mathcal{R}$ provides the spatial framework for avatar movement and real-world interaction. Movement errors often arise from **attitude misalignment** between the **body schema** and the visually-derived **environment schema** (the two main components of $\mathcal{R}$). For example, a **yaw error** in the body schema—where it is assumed to be rotated slightly clockwise (bird's-eye view) from its actual position relative to the visually perceived refrigerator—results in an underreach when grasping the handle. The arm is miscalculated as being closer to the target than it actually is, despite correct trajectory planning.

2.3 Imaginal schema ($\mathcal{I}$): 3D non-veridical workspace w/ Sim(3) action

The imaginal schema $\mathcal{I}$ provides a dynamic volumetric overlay to the real schema $\mathcal{R}$, serving as a workspace for non-veridical spatial representation and reasoning. Key properties include:

- **Functional scope**: Generates hypothetical situations, warning imagery (e.g., potential bitten-finger flash when bringing fingers into mouth while eating chips to induce caution), memories, conceptual contemplation, action simulations, and dream content,
- **Viewing perspective**: Typically observed by a "mind's eye" that can orbit and relocate (and $\mathcal{I}$ itself can rapidly zoom) independently of the avatar's cyclopean eye in $\mathcal{R}$, though dreams and certain cases may embed a "mind's avatar" within $\mathcal{I}$,
- **Dynamic interaction**: Frequent switching between $\mathcal{R}$ and $\mathcal{I}$ occurs during normal cognition, with $\mathcal{I}$ serving as a temporary workspace before returning to reality-based processing,
- **Display dominance**: While often overlaying $\mathcal{R}$, $\mathcal{I}$ can fully dominate conscious frames, creating anticorrelated periods of purely imaginal or real experience,
- **Volumetric scaling**: Objects are dynamically rescaled relative to $\mathcal{R}$ with extreme rapidity—comparable to the fastest camera zoom—frequently enlarging small elements for detailed inspection,
- **Variable visibility**: Ranges from completely transparent to vivid and photorealistic, with individual differences in conscious access—some experience $\mathcal{I}$ as plain as day while others have little visual awareness,
- **Non-veridical content**: Supports imagined, remembered, or potential future geometries—places, times, and scenarios not matching to $\mathcal{R}$,
- **Geometric utility**: Maintains full spatial functionality regardless of visibility, enabling both conscious inspection and "blindsight"-style geometric processing.

Unlike the action-oriented $\mathcal{R}$, $\mathcal{I}$ serves as a flexible workspace where metacognition operates as observer of non-literal geometric content. It is possible to have more than one $\mathcal{I}$ at once.

2.4 Time schema ($\mathcal{T}$): 3D flowfield and fading buffer w/ Sim(3) action

$\mathcal{T}$ stores recent prints as a fading temporal stack, producing the *illusion of continuity* via overlap of access windows:

- **Ringframe sequencing**: fading history of recent $\rho(\tau)$ over $\tau \in [t-\Delta, t]$ yields continuity.
- **Multi-modal timing**: supports both continuous phasic scanning and discrete interrupts.
- **Dynamic cadence**: governed by competition between baseline rhythm $\beta(t)$ and mic events.

Conscious "printing" is the act of the operator Π sampling on $\mathcal{A}$:

$$\rho(t) = \Pi(\mathcal{A}(t), S, g(t)), \qquad \mathcal{A}(t) \subseteq \mathcal{B}, \qquad \rho(t) \hookrightarrow \mathcal{T}.$$

$\mathcal{T}$ functions as a fading stack or flowfield of recent ρ printed by Π on $\mathcal{A}$, yielding apparent continuity from discrete acts of access. The activity of Π may follow either of two drives: a transient, high-level mic signal $\mathcal{M}(t)$ conveying structured content, or an endogenous baseline rhythm $\beta(t)$ maintained by refractory dynamics when $\mathcal{M}(t)$ is silent. Thus,

$$\Pi(t) = \begin{cases} f(\mathcal{M}(t)), & \text{if mic-driven,} \\ \beta(t), & \text{if silent or quiescent.} \end{cases}$$

This mic-vs-baseline distinction concerns the *drive* behind printing; independently, Π operates in distinct temporal *modes* (phasic, compressed phasic, interrupt, extrusion) that determine *how*

$\mathcal{A}$ is sampled over time (see §5). Phasic modes correspond to continuous modulation of $\beta(t)$ by $\mathcal{M}(t)$, whereas interrupt modes reflect discrete, hazard-scheduled prints. Both contribute to the ongoing flowfield of $\mathcal{T}$, which merges the outputs of Π into a seemingly continuous conscious stream.

2.5 Real $\mathcal{R}$ and imaginal $\mathcal{I}$ are readouts with latency

We treat $\mathcal{R}$ (veridical, action-oriented) and $\mathcal{I}$ (non-veridical, constructive) as readouts integrating recent prints:

$$[\mathcal{R}(t), \mathcal{I}(t)] := f\left(\int_{t-\Delta}^{t} G(t-\tau)\,[\rho(\tau), \mathcal{R}(\tau), \mathcal{I}(\tau)]\,d\tau\right), \tag{2}$$

with a causal kernel G. Vividness and rapid zooms reflect gain and Sim(3) pose control over IT/PPC codes. $\mathcal{I}$ may overlay or dominate $\mathcal{R}$.

2.6 Access manifold ($\mathcal{A}$, 0–2D) and display ($\mathcal{D} = \mathcal{U}_{\text{struct}}$)

We distinguish the *structural union* (full conscious display, union of schemas on manifold)

$$\mathcal{U}_{\text{struct}}(t) := \mathcal{B}(t) \cup \mathcal{R}(t) \cup \mathcal{I}(t) \cup \mathcal{T}(t) \tag{3}$$

from the *operational access manifold* (intersection of schemas)

$$\mathcal{A}(t) := \mathcal{B}(t) \cap \mathcal{R}(t) \cap \mathcal{I}(t) \cap \mathcal{T}(t), \qquad \mathcal{A}(t) \subseteq \mathcal{B}. \tag{4}$$

$\mathcal{U}_{\text{struct}}$ is everything in the display; $\mathcal{A}$ is what is *touched* between schemas—a subset of $\mathcal{B}$ that often exhibits a graded excitability or printing potential, sometimes spreading radially from a central focus outward across the bank. We refer to $\mathcal{U}_{\text{struct}}$ and $\mathcal{D}$ interchangeably as the *conscious display*.

2.7 Ringframes (ρ): 0–2D fading manifolds

A ringframe $\rho(t)$ is material printed by the operator Π on the access manifold $\mathcal{A}$ into the time schema $\mathcal{T}$. It is the basic unit of conscious access, bridging $\mathcal{B} \to \mathcal{A} \to \mathcal{T}$.

- **Ring:** 0–1D print — a tracer following a path or the instantaneous print of that path.
- **Frame:** 2D print — access activity that sweeps or fills an area of $\mathcal{A}$ over time, whether all at once or by motion.

Both are printed from the Bank $\mathcal{B}$, posed by $g(t) \in \text{Sim}(3)$, and deposited in $\mathcal{T}$ as a record. Phasic modes yield seamless cycles (helices in $\mathcal{T}$), compressed phasic modes yield lock-washer type geometries in $\mathcal{T}$, and interrupt modes produce discrete frames in $\mathcal{T}$. Square trajectories; swept or extruded contours; unclosed V, U or linear manifolds (as trajectories or swept contours); etc.; are all still considered ringframe material, since they arise from the same act of printing by Π on $\mathcal{A}$ into $\mathcal{T}$. As hippocampal patients retain immediate present context, it is *not* thought that the time schema/ringframes are instantiated by the HPC, although the greater HPC (including EC), RSP, and DMN (including ACC/mPFC) *might* be at play.

A **card** is a ringframe produced during one sweep of a microcycle (see §5). Cards are the discrete, interrupt-like "blips" of access that tile the macrocycle in rolodex and paddlewheel regimes.

2.8 Printing operator (Π): sampling the access manifold $\mathcal{A}$

The printing operator Π samples the access manifold $\mathcal{A}$ and deposits ringframe material ρ into the time schema $\mathcal{T}$. It operates in distinct temporal *modes*—phasic, compressed phasic, interrupt, and extrusion—that determine how $\mathcal{A}$ is sampled over time (§5). Its *drive* may be either mic-signal $\mathcal{M}(t)$ or baseline rhythm $\beta(t)$ (§2, Time Schema). When Π operates in a rhythmic regime, its printing cadence (instantaneous frequency, phase, and duty cycle) admits temporal derivatives $\dot{\Pi}, \ddot{\Pi}, \ldots$ up to order $L \approx 3$–5, allowing the system to feel and deliberately steer intra-cycle variations (e.g., phase-eating, frequency chirps, or duty-cycle sweeps).

2.9 Mic signal ($\mathcal{M}$), voice ($\vec{C}$), and baseline rhythm (β)

The printing operator Π is primarily driven by the high-level mic signal $\mathcal{M}(t)$, guided by the aboutness vector $\vec{C}(t)$, and sustained in silence by the baseline rhythm $\beta(t)$.

- **Mic signal $\boldsymbol{\mathcal{M}(t)}$:** A transient, structured drive carrying any high-level events of consciousness. $\mathcal{M}(t)$ modulates the printing operator Π, producing organized ringframes that embody current goals, percepts, or thoughts. It is the amplitude envelope (if present) of any active "voice" aboutness vector (if present).
- **Voice (aboutness vector $\boldsymbol{\vec{C}(t)}$):** A directional vector in concept space that is what $\mathcal{M}(t)$ and $\beta(t)$ are about. $\vec{C}(t)$ governs *what* the system is about, biasing both $\mathcal{M}(t)$ and $\beta(t)$ toward the appropriate conceptual or perceptual surface within $\mathcal{D}$.
- **Baseline rhythm $\boldsymbol{\beta(t)}$:** An endogenous oscillation emerging from refractory dynamics, maintaining access continuity when $\mathcal{M}(t)$ is quiescent. $\beta(t)$ provides the rhythmic substrate on which $\mathcal{M}(t)$ rides, filling silent periods with spontaneous prints that preserve temporal coherence in $\mathcal{T}$. $\beta(t)$ provides a silent, slow (2–7 Hz) frame rate of dream and daydream imagery (which may also use $\mathcal{M}(t)$).

In concert, $\mathcal{M}(t)$ provides structure, $\vec{C}(t)$ supplies intent, and $\beta(t)$ sustains a minimal frame rate—together orchestrating the ongoing printstream of consciousness.

2.10 Observer cameras ($\Xi_{\textbf{Cyclopean}}$, $\Xi_{\textbf{Mind's Eye}}$)

The two conscious viewpoints are modeled as infinitesimal point cameras with full SE(3) freedom. $\Xi_{\text{Cyclopean}}$ represents the fused avatar or "real" eye within $\mathcal{R}$, while $\Xi_{\text{Mind's Eye}}$ represents the internally oriented "imaginal" eye within $\mathcal{I}$. Each camera defines a right-handed coordinate frame with orthonormal basis vectors for gaze, up, and left:

$$\Xi_{\text{Cyclopean}}, \Xi_{\text{Mind's Eye}} \in \text{SE}(3), \qquad \{\vec{g}, \vec{u}, \vec{l}\} = (\text{gaze, up, left}).$$

Together, these provide the perspective impingement operators through which $\mathcal{R}$ and $\mathcal{I}$ are viewed within the conscious display $\mathcal{D}$.

3 Physics modeling, schema/camera posing, and perspective

The conscious display $\mathcal{D}$ (or $\mathcal{U}_{\text{struct}}$) integrates three geometric streams: **Physics**—the inferred 3D world in $\mathcal{R}$; **Perspective**—the SE(3) camera pose; **Pose**—the Sim(3) overlay of Bank and Imaginal schemas. These determine what is seen, from where, and how internal volumes are scaled and placed.

3.1 Physics modeling and schema/camera posing

In computer animation, object physics (an apple falling) and camera scene-framing (orbiting around it) are separate elements jointly linked by keyframes. Similarly, the brain must reify raw signals into physical geometry, position the self-model at a viewpoint, and "pose" the overlay of mental imagery at a specific location, orientation, and scale (the posing is a Sim(3) action on $\mathcal{I}$). Finally, any ongoing aboutness stream is able to exert coordinated modulation on baseline behaviors (of bank, imagination, printing operator timing/modes, selection of $\mathcal{A}$, behavior output, etc.). The conscious display $\mathcal{D}$ (equivalently $\mathcal{U}_{\text{struct}}$) is the integrated result of baseline defaults and any coordinated modulation by the aboutness vector $\vec{C}(t)$. The posing of $\mathcal{B}$, $\mathcal{I}$, $\Xi_{\text{Cyclopean}}$, $\Xi_{\text{Mind's Eye}}$, etc., are governed by a small set of Lie groups acting on Euclidean space, shown in Table 1.

Table 1: Principal geometric groups governing schema posing and display composition.

Group	**Action**	**Functional Role in Display**
$\mathbf{SO(2)}$	Planar rotation in $\mathbb{R}^2$	Azimuthal orientation within ringframes.
$\mathbf{Sim(2)}$	2D rotation, translation, uniform scaling	Projection planes (retinal/imaginative slices).
$\mathbf{SO(3)}$	3D rotation	Orientation of body, head, gaze.
$\mathbf{SE(3)}$	3D rotation and translation	Pose of real and mind's eye cameras.
$\mathbf{Sim(3)}$	3D rotation, translation, uniform scaling	Bank/imaginal embedding and relative scale.

Sim(3) sets global placement; SE(3) moves cameras within posed spaces. A radiance sphere $L(\omega, \nu)$ describes physical input, while $L_{\text{perc}}(\omega)$ encodes solved perceptual color/intensity per direction, shared by $\mathcal{R}$ and $\mathcal{I}$.

3.2 Camera perspective (radiance)

In addition to geometric transformations, the **radiance sphere** $L(\omega, \nu)$ represents the directional and frequency-dependent energy distribution over the unit sphere of orientations $\omega \in \mathbb{S}^2$ and spectral domain ν. This quantity captures the angular structure of visual illumination and serves as the input to derive painted detail (*paint*) within the posed $\mathcal{R}$ schema.

$$L_{\text{phys}}(\omega, \nu) : \mathbb{S}^2 \times \mathbb{R}^+ \to \mathbb{R}^+, \tag{5}$$

Symbol	Meaning
L_{phys}	Radiance — the amount of light per unit area, per direction, and per frequency
ω	A direction on the unit sphere $\mathbb{S}^2$ (a vector pointing outward from the eye or sensor)
ν	Frequency of light in hertz (sometimes expressed as wavelength λ in meters)
$\mathbb{S}^2 \times \mathbb{R}^+$	Domain: all viewing directions (unit sphere) $\times$ all positive frequencies
$\mathbb{R}^+$	Range: a single positive real value — radiance in watts$\cdot$m$^{-2}\cdot$sr$^{-1}\cdot$Hz^{-1}

Perceptually, the 2-D visual field of $\mathcal{R}$ or $\mathcal{I}$ consists of a single color (derived from a 3D opponent-color manifold of H/S/B) and intensity for any solid angle ω.

$$L_{\text{perc}}(\omega) : \mathbb{S}^2 \to \mathbb{C}_{\text{perc}} \times \mathbb{R}^+, \tag{6}$$

Symbol	Meaning
L_{perc}	Perceptual radiance — the *conscious* color and intensity assigned to direction ω
ω	A direction on the perceptual sphere $\mathbb{S}^2$ (each ray of conscious visual space)
$\mathbb{C}_{\text{perc}}$	The perceptual color space (e.g., a 3D opponent-color manifold of hue, saturation, brightness)
$\mathbb{S}^2$	Domain: all perceptual ray directions in the conscious field
$\mathbb{C}_{\text{perc}} \times \mathbb{R}^+$	Range: one perceived color and intensity for each direction

Table 2: Camera reference frames and their associated radiance fields.

Level	Camera	Field
Physical	*Retinal Camera* (biological eyes)	$L_{\text{phys}}(\omega, \nu)$ — physical radiance: intensity as a function of viewing direction $\omega \in \mathbb{S}^2$ and frequency $\nu \in \mathbb{R}^+$. Represents incoming spectral energy (intensities of red through violet) before any cortical processing.
Perceptual (External Scene)	*Cyclopean Camera* (fused-avatar eye)	$L_{\text{perc}}(\omega)$ — perceptual radiance: the solved percept for each direction ω, i.e. one experienced color and brightness value derived from external sensory input.
Perceptual (Internal Scene)	*Imaginal Camera* (mind's eye)	$L_{\text{perc}}(\omega)$ — same perceptual format (color and brightness per direction), but sourced from internally generated schema geometry rather than current retinal input.

L_{phys} is the physical spectral input, while L_{perc} is the unified perceptual radiance field for both externally grounded and internally generated scenes ($\mathcal{R}$ and $\mathcal{I}$). The Cyclopean and mind's eyes can each be modeled as infinitesimal point cameras embedded in the conscious display, possessing full SE(3) freedom with defined up, gaze, and left vectors for capturing perspective views from $\mathcal{R}$ and/or $\mathcal{I}$.

(1) The spatial inverse problem: the eyes receive two-dimensional radiance patterns, yet the system must reify a three-dimensional world as their cause. Each retinal image is an array of directions ω whose depth structure must be inferred as reified source/altering objects within the real schema $\mathcal{R}$.

(2) The color inverse problem: light from a distal surface (e.g. brown wallpaper) may pass through multiple semi-transparent layers—such as two layers of green glass from a Coke bottle and two of a red balloon—before reaching the eyes. V1 arrives at a single mixed color and intensity for that direction, yet the visual system must recover and assign distinct colors to the reified objects responsible for the mixture: the red balloon, the green Coke bottle, and the brown wall. This is analogous to cel animation rendered in three dimensions: each layer (wall, Coke bottle, balloon) contributes to the final pixel but retains its own object-attached color property in the reconstructed scene.

(3) Perspective color vs. object color: in the conscious display, each viewing direction ω carries only one apparent color and intensity; but in the reified real schema $\mathcal{R}$, multiple voxel locations along that ray—sometimes five or more—each possess their own color property anchored to object meaning and depth.

4 Aboutness modulation and multidimensional control

The Bank $\mathcal{B}$ operates under rhythmic baseline behaviors (stationary, revolving, or bobbing), which maintain ongoing Sim(3) motion and spatial coherence. Superimposed upon these baselines is a multidimensional modulation envelope governed by an *aboutness vector* $\vec{C}(t)$ that coordinates pose, timing, and access across all active schemas.

4.1 Bank baseline behaviors and modulation envelope

1. **Stationary:** Fixed Sim(3) pose requiring explicit $\mathcal{T}$ schema stabilization.
2. **Orbit/Rotation (primary):** Continuous Sim(3) motion with toroidal geometry—manifesting as *pure rotation*, *spirographic rolling*, or *tidally locked orbit*—with major radius ranging from compact (tight spirograph) to extended (torus-scale) trajectories. Cylinder, sphere, and cone variants of spirographic behavior may occur.
3. **Bobbing:** Hybrid oscillation coupling dominant slow scale-drift with intermittent rapid inertial transients, analogous to (1) seaweed undulating in tidal currents, or (2) a buoy on quiet water subject to slow drifts in various directions, punctuated by intermittent sharp jostles, a result of surface and subsurface fluctuations.

4.2 Modulated bank behaviors and emergent dynamics

Superimposed upon the baseline cadences is a suite of aboutness-driven modulations that deform the Bank's Sim(3) trajectory, intra-bank walks, and access timing. These modulated states arise when $\vec{C}(t)$ couples strongly to specific perceptual, interoceptive, or kinematic signals:

1. **Object-Lock (Real-Time Pose Tracking):** When attention fixates on a physical object (e.g., an iPhone held in hand), the Bank dynamically "glues" its reference geometry to the target, continuously tracking $g(t)$, $\dot{g}(t)$, and $\ddot{g}(t)$ in real time. The Bank's *cylinder* aligns to the object's frame, making spatial tracking feel bound to the target rather than visually estimated. Pose updates propagate through the access manifold $\mathcal{A}$, ensuring seamless Sim(3) coupling between external object and internal display. For tracking a rolling ball, the Bank's *sphere* would align.

2. **Kinematic Qualia Encoding (Emergent Visual/Somatic Resonance):** Sustained interoceptive or affective states spontaneously map onto Bank kinematics without peripheral actuation, manifesting as: (i) *Reciprocation*—rapid back-and-forth oscillation (sawzall-like) of the Bank cylinder during photic entrainment, where parallel zigzag/chevron walls oscillate between left- and right-tilt attractors at 2–6 Hz. The transition may preserve color ordering or flip it (Fig. 13), often with shrinking inter-line spacing, increasing frequency, fading opacity, and 90° attractor shifts which would form an X-pattern of the centermost zigzag line from the two bistable epochs; and (ii) *Qualia Instantiation*—non-visual sensations encoded via geometric resonance, e.g., "shivering cold" instantiated as the Bank oscillating $\sim$5 Hz between torso and shoulder regions for ~ 2 s. Incidentally, this use case is also another exemplar of reciprocation. The qualia is felt *because* the Bank moves that way, rendered in a geometro-spatio-spectral manner despite zero physical movement.

3. **Inertial "Throw" (Acceleration Aboutness):** Sudden changes in physical acceleration are rendered as a transient SE(3) perturbation of the Bank and Access Manifold. For instance, when a driver turns sharply left, the conscious display registers a compensatory "throw" of $\mathcal{A}$ and $\mathcal{B}$ rightward and/or upward within $\mathcal{R}$. This is not a delayed reaction but an immediate, hazard-gated kinematic offset that re-sites $\mathcal{A}$ to encode and correlate with that force.

4. **"Vibes" (Amplitude Envelope Modulation):** Rhythmic or textured sensory inputs (e.g., snare hits, vocal onsets, pitch) modulate the amplitude envelope of Bank dynamics. These "vibes" do not alter mean pose but instead drive continuous, phasic adjustments to pose, such as $\mathcal{B}$'s/$\mathcal{A}$'s scale, frequency, attitude, or intensity in $\mathcal{R}$. The effect binds auditory or textural qualia to spatial cadence, smoothly deforming the access window without interrupting the underlying baseline trajectory.

These modulated behaviors demonstrate that aboutness does not merely shift attentional focus; it directly warps the Sim(3) geometry, temporal derivatives, and access timing of the Bank, producing phenomenologically distinct kinematic signatures that can be tracked, predicted, and linked to hazard-gated printing.

4.3 Independent pose-jet control

The Sim(3) pose $g(t) = \big(s(t), R(t), t(t)\big)$ governing Bank and Imaginal schema display decomposes into seven control degrees: three translational ($t_x, t_y, t_z \in \mathbb{R}^3$), three rotational (parameterizing $R \in \mathrm{SO}(3)$), and one uniform scale ($s \in \mathbb{R}^+$). Critically, these degrees operate under *independent temporal modulation*:

1. **Cross-schema independence:** Bank pose $g_{\mathcal{B}}(t)$ and Imaginal pose $g_{\mathcal{I}}(t)$ evolve under distinct control signals. The Bank may undergo slow, stabilizing drift while $\mathcal{I}$ executes rapid zooms or orbital sweeps, or vice versa.

2. **Intra-pose independence:** Within a single $g(t)$, translation $t(t)$, rotation $R(t)$, and scale $s(t)$ follow separable trajectories. For example, scale may chirp ($\dot{s} \neq 0$) while orientation remains locked ($\dot{R} \approx 0$), or position may track a target while scale holds steady.

Beyond instantaneous pose, the *jet* of temporal derivatives carries control information:

$$J_g^{(K)}(t) := \{g^{(k)}(t)\}_{k=0}^{K} = \{g(t), \dot{g}(t), \ddot{g}(t), \ldots, g^{(K)}(t)\}, \tag{7}$$

where $g^{(k)} = d^k g/dt^k$. While the mathematical jet is infinite, neural precision and biomechanical bandwidth likely restrict effective control to $K \approx 4$–5 (position through snap/jounce). To handle derivatives rigorously, we pull them back to the Lie algebra $\mathfrak{sim}(3)$ via left-translation for control and extrapolation.

The aboutness vector $\vec{C}(t)$ modulates this jet through a control field $\mathcal{F}$:

$$J_g^{(K)}(t) = \mathcal{F}\big(\vec{C}(t), J_g^{(K)}(t-\delta), \text{context}\big), \tag{8}$$

allowing intentional focus to shape not just *where* a schema is posed, but *how* it moves—its velocity profile, acceleration curvature, and higher-order kinematic texture. This jet-level control underlies phenomenological distinctions such as "smooth zoom" vs. "jump-cut", or "steady orbit" vs. "tremulous hover".

These baselines are continuously deformed by a modulation envelope acting through three control domains, each specifiable via pose-jet structure $J_g^{(K)}$ (with derivative components pulled back to $\mathfrak{sim}(3)$ for control):

$$\textbf{Pose adjustment:} \quad \Delta J_g^{(K)}(t) \in J^K(\mathbb{R}, \mathrm{Sim}(3)), \tag{9}$$

$$\textbf{Intra-bank walk/shape-shift:} \quad \mathcal{A}_{\text{shift}}(t) \subset \mathcal{B}, \tag{10}$$

$$\textbf{Temporal synchronization:} \quad t_{\text{align}} = \arg\min_t \|\mathcal{B}(t) - \vec{x}_{\text{target}}\|. \tag{11}$$

where:

- **Pose adjustment** steers not just pose but velocity/acceleration profiles (via pullback to $\mathfrak{sim}(3)$);
- **Intra-bank walk/shape-shift** may include optional temporal derivative constraints on the walk trajectory;
- **Temporal synchronization** can optionally match jet terms for smooth handoff.

The printing operator Π samples $\mathcal{A}$ using the pose $g_{\text{eff}}(t)$, which is *treated as present* by the conscious system:

$$g_{\text{eff}}(t) \approx g(t_{\text{sense}}) \exp\Big(\tau_{\text{lat}}\, \xi(t_{\text{sense}}) + \tfrac{1}{2}\tau_{\text{lat}}^2\, \dot{\xi}(t_{\text{sense}}) + \cdots\Big), \tag{12}$$

where $t_{\text{sense}} = t - \tau_{\text{lat}}$ and $\exp : \mathfrak{sim}(3) \to \mathrm{Sim}(3)$ reconstructs pose from body-frame motion generators. Crucially, $g_{\text{eff}}(t)$ is not a forecast or a "best guess"—it is the pose used for access *as if* it were aligned with external present. The hazard function $h(t)$, the selection of $\mathcal{A}$, and the operation of Π all reference this internal present. Motor commands are issued $\sim$130 ms before intended action onset: $\sim$30 ms to compensate for the internal model's perceptual latency, and $\sim$100 ms to overcome peripheral delays in neuromuscular transmission and muscle activation. The "paint" layer (L_{perc}, color/intensity/content assignment of $\mathcal{R}$ and $\mathcal{I}$) operates with additional latency and can autocomplete forward or backward in time; but the *when* of access—the hazard-gated printing of ρ into $\mathcal{T}$—is treated as temporally immediate.

4.4 Orbital parameter jets

When the Bank operates in revolving/orbital mode, the macrocycle trajectory is parameterized by orbital elements that themselves admit independent jet modulation. The orbital state is not

simply a consequence of $g_{\mathcal{A}}(t)$ but is governed by a separate set of control parameters:

$$\omega_{\text{orb}}(t) \quad \text{(orbital angular frequency, typically 0.5–13 Hz)}, \tag{13}$$
$$r_{\text{orb}}(t) \quad \text{(orbital radius/major axis)}, \tag{14}$$
$$\hat{n}_{\text{orb}}(t) \in \mathbb{S}^2 \quad \text{(orbital plane normal vector)}, \tag{15}$$
$$\phi_{\text{orb}}(t) \quad \text{(orbital phase)}, \tag{16}$$
$$e_{\text{orb}}(t) \quad \text{(eccentricity, for non-circular orbits)}. \tag{17}$$

Each orbital parameter admits its own temporal jet up to order $N \approx 4$–5:

$$J_{\omega}^{(N)}(t) = \{\omega_{\text{orb}}, \dot{\omega}_{\text{orb}}, \ddot{\omega}_{\text{orb}}, \dots\}, \quad J_{r}^{(N)}(t) = \{r_{\text{orb}}, \dot{r}_{\text{orb}}, \ddot{r}_{\text{orb}}, \dots\}, \quad \text{etc.} \tag{18}$$

Phenomenologically, this allows the system to modulate not just *where* the Bank is in its orbit, but *how the orbit itself evolves*: orbital frequency chirps ($\dot{\omega}_{\text{orb}} \neq 0$), radius breathing ($\dot{r}_{\text{orb}} \neq 0$), orbital plane precession ($\dot{\hat{n}}_{\text{orb}} \neq 0$), and eccentricity modulation. In practice, ω_{orb} is often held nearly constant (stable spirographic cadence), but can be deliberately swept during attentional transitions or photic entrainment. The orbital jet $J_{\text{orb}}^{(N)}$ is slaved to the aboutness vector $\vec{C}(t)$ and couples to the pose jet $J_{g_{\mathcal{A}}}^{(K)}$ through the mapping $\Phi_{\mathcal{R}_{\text{A}} \to \mathcal{A}}$.

4.5 Coordinated aboutness field

Aboutness is represented by a vector $\vec{C}(t)$ in concept space, but functionally behaves as a global control field synchronizing multiple geometric systems. It jointly modulates:

- The Sim(3) pose of the **Imaginal schema** $\mathcal{I}$ (scale, 3D orientation, and translation);
- The Sim(3) pose of the **Bank** $\mathcal{B}$, adjusting the reference geometry.
- The **selection** of the access manifold $\mathcal{A}$, which also fixes the effective Sim(3) pose of $\mathcal{T}$, and the **timing** of operations by Π.
- The **mode and signal** of the printing operator Π (phasic, compressed phasic, interrupt, or extrusion), determining how ringframes $\rho(t)$ materialize in $\mathcal{T}$.
- The **head/eye turns** of the avatar (and of the mind's avatar, when present as a non-servo, pretend body schema in $\mathcal{I}$), and **orbits, jumps**, and other exotic behaviors of the mind's eye. All of these are examples of dynamic SE(3) posing of head and $\Xi_{\text{Cyclopean}}$ and $\Xi_{\text{Mind's Eye}}$.
- **Jump-cuts** and **orbital cross-fades** between $\mathcal{R}$ and $\mathcal{I}$ (as facilitated by $\Xi_{\text{Cyclopean}}$ and $\Xi_{\text{Mind's Eye}}$), and varying opacity overlays of $\mathcal{I}$ visible to $\Xi_{\text{Cyclopean}}$.

Thus, $\vec{C}(t)$ orchestrates simultaneous modulation across all these manifolds, binding pose, access, and printing into a unified act of reference.

4.6 Capture dynamics and timescales

$$\Delta g(t) = f(\vec{C}, t), \qquad \vec{C} \in \text{Concept Space}. \tag{19}$$

Capture timescales:

- **Short-term (Keyframing):** Rapid modulations (100–500 ms) in "mic voice" (aboutness) — e.g., hand gesture shifts, driving gaze changes, cooking task transitions.
- **Long-term (Locked capture):** Sustained alignment (seconds) — e.g., tracking an object, watching a performer, or following a melody.

4.7 Unified control formulation

Baseline dynamics integrate with aboutness-driven modulation as:

$$\textbf{Baseline:} \quad \mathcal{B}_{\mathcal{D}} = g_{\mathcal{D}}(\mathcal{B}), \tag{20}$$

$$\textbf{Modulated:} \quad \mathcal{B}_{\mathcal{D},\mathrm{mod}}(t) = \mathcal{B}_{\mathcal{D}} + \Delta g(\vec{C}, t), \tag{21}$$

$$\textbf{Aboutness:} \quad \vec{C} = \begin{cases} \text{Top-down: intentional focus, self/goal-driven} \\ \text{Bottom-up: sensory salience or hazard-driven.} \end{cases} \tag{22}$$

4.8 Hierarchical system dynamics and pose coupling

Contrary to a flat state-vector formulation, conscious dynamics follow a *hierarchical mapping-coupling* architecture anchored in the peripersonal reference frame of the Real Schema Avatar $\mathcal{R}_{\mathrm{A}}$ (an $\sim 8'$ cubic volume encoding the sense of self-in-space). Even prior to conscious printing, $\mathcal{R}_{\mathrm{A}}$ maintains a baseline phenomenology of 3D blackness, a stable sense of up/down, and a fixed ego-centric viewpoint from the "back" of the volume looking outward. $\mathcal{A}$ maintains a voxel-to-voxel "marriage" (spatial correspondence) relative to this reference (and $\mathcal{B}$, $\mathcal{R}$, and $\mathcal{I}$ maintain voxel-to-voxel marriages to $\mathcal{A}$); the rigidity and control of these mappings differ fundamentally:

$$\Phi_{\mathcal{R}_{\mathrm{A}}\to\mathcal{A}}(t) \quad \text{(primary/first-level dynamic mapping)}, \tag{23}$$

$$\Phi_{\mathcal{A}\to\mathcal{B}}(t),\ \Phi_{\mathcal{A}\to\mathcal{R}}(t),\ \Phi_{\mathcal{A}\to\mathcal{I}}(t) \quad \text{(secondary mappings slaved to } \mathcal{A}). \tag{24}$$

The Access Manifold pose $g_{\mathcal{A}}(t) \in \mathrm{Sim}(3)$ is not a primitive degree of freedom; it is the kinematic projection of $\Phi_{\mathcal{R}_{\mathrm{A}}\to\mathcal{A}}(t)$ and constitutes the first-level mapping that drives all downstream schema poses. Crucially, attention shifts (when shape/location of $\mathcal{A}$ within $\mathcal{B}$ is held constant) are achieved by *rewiring the $\mathcal{A}$–$\mathcal{R}$ marriage* while preserving the $\mathcal{A}$–$\mathcal{B}$ marriage. For example, shifting attention from a pen on the left to an identical pen on the right requires no intra-bank walk and no change in $\mathcal{A}$'s pose relative to $\mathcal{B}$; instead, $\Phi_{\mathcal{R}_{\mathrm{A}}\to\mathcal{A}}(t)$ dynamically remaps $\mathcal{A}$'s voxels to new locations in $\mathcal{R}_{\mathrm{A}}$ (and thus to new voxels in the stable $\mathcal{R}$), instantaneously re-siting conscious access as well as the entire Bank $\mathcal{B}$.

Because $\mathcal{B}$, $\mathcal{R}$, and $\mathcal{I}$ are coupled to $\mathcal{A}$ (second-level mappings), their full pose jets are *instantiated via mapping derivatives*:

$$J_{g_\cdot}^{(K)}(t) = \left\{ \frac{d^k}{dt^k} \Phi_{\mathcal{A}\to\cdot}\big(g_{\mathcal{A}}(t), \vec{C}(t)\big) \right\}_{k=0}^{K}, \quad \cdot \in \{\mathcal{B}, \mathcal{R}, \mathcal{I}\}, \tag{25}$$

meaning velocity, acceleration, and higher-order kinematic texture emerge directly from the instantaneous deformation rate of the coupling maps themselves. This mapping orchestration operates with sub-millisecond temporal precision, allowing the system to seamlessly transition between rigid lock-on (e.g., sedated passenger rings tracking vehicle yaw while ignoring body motion) and free orbital drift (e.g., $\mathcal{A}$ taking a cyclic orbit around $\mathcal{R}$) without kinematic discontinuity or temporal lag. Stability profiles reflect mapping rigidity: $\Phi_{\mathcal{A}\to\mathcal{R}}$ is heavily constrained, yielding $\dot{g}_{\mathcal{R}} \approx 0$ and a stable servo reference for action, whereas $\Phi_{\mathcal{A}\to\mathcal{B}}$ and $\Phi_{\mathcal{A}\to\mathcal{I}}$ are highly deformable, producing the continuous, non-stationary drift characteristic of baseline cadence and aboutness modulation.

The printing operator Π and observer cameras Ξ operate on distinct mathematical manifolds and admit their own temporal jets, both ultimately instantiated via mappings:

- **Printing operator Π:** Not a Sim(3) object. Π is a temporal/intensity modulation channel governed by gain envelopes, adaptive noise thresholds, and temporal binning. It sometimes maps each of several bins onto angular sectors (0–360°) of $\mathcal{A}$, an arbitrary division of time into bins where phase of bin maps to phase of manifold. In interrupt mode, activation is

strictly gated by the hazard function $h(t)$. As noted in §2, when Π operates in a rhythmic regime, its printing cadence admits derivatives $\dot{\Pi}, \ddot{\Pi}, \ldots$ up to $L \approx 3$–5, allowing the system to feel and deliberately steer intra-cycle variations (e.g., phase-eating, frequency chirps, or duty-cycle sweeps) rather than treating them as fixed parameters.

- **Observer cameras Ξ:** Pure SE(3) viewpoint operators. They sample the posed display without scale coupling, maintaining independent gaze, up, and left vectors for cyclopean and mind's-eye perspectives. Viewpoint trajectory is not static; $\Xi(t)$ admits a full viewpoint jet $J_{\Xi}^{(M)}(t) = \{\Xi^{(m)}(t)\}_{m=0}^{M}$ with $M \approx 3$–5. This jet is instantiated via a perspective mapping: centering a Bank copy at the cyclopean or mind's-eye pupil projects perspective rays onto lines of voxels, such that gaze shifts, orbital tracking, and anticipatory movements emerge from the time-varying derivatives of this projection map rather than independent kinematic integration.

Because $\mathcal{B}$, $\mathcal{R}$, and $\mathcal{I}$ are algebraically slaved to the first-level mapping $\Phi_{\mathcal{R}_{\mathrm{A}} \to \mathcal{A}}$ (and its derivatives) via these secondary couplings, and Π's temporal envelope plus Ξ's viewpoint trajectory are independently jet-modulated via second-level mappings, the independent dynamical state reduces to the pose jet, cadence jet, viewpoint jet, and mapping drivers. The system evolves under the competition between aboutness-driven modulation and attractor-state inertia:

$$\frac{d}{dt}\begin{bmatrix} g_{\mathcal{A}} \\ \dot{g}_{\mathcal{A}} \\ \vdots \\ g_{\mathcal{A}}^{(K-1)} \\ \omega_{\mathrm{orb}} \\ \dot{\omega}_{\mathrm{orb}} \\ \vdots \\ \omega_{\mathrm{orb}}^{(N-1)} \\ r_{\mathrm{orb}} \\ \dot{r}_{\mathrm{orb}} \\ \vdots \\ r_{\mathrm{orb}}^{(N-1)} \\ \Pi \\ \dot{\Pi} \\ \vdots \\ \Pi^{(L-1)} \\ \Xi \\ \dot{\Xi} \\ \vdots \\ \Xi^{(M-1)} \end{bmatrix} = \alpha\, F_{\mathrm{drive}}\big(\vec{C}(t),\, h(t),\, J_{\Phi},\, J_{\mathrm{orb}}^{(N)}\big) + \gamma\, H_{\mathrm{inertia}} \left(\begin{bmatrix} g_{\mathcal{A}} \\ \dot{g}_{\mathcal{A}} \\ \vdots \\ g_{\mathcal{A}}^{(K-1)} \\ \omega_{\mathrm{orb}} \\ \dot{\omega}_{\mathrm{orb}} \\ \vdots \\ \omega_{\mathrm{orb}}^{(N-1)} \\ r_{\mathrm{orb}} \\ \dot{r}_{\mathrm{orb}} \\ \vdots \\ r_{\mathrm{orb}}^{(N-1)} \\ \Pi \\ \dot{\Pi} \\ \vdots \\ \Pi^{(L-1)} \\ \Xi \\ \dot{\Xi} \\ \vdots \\ \Xi^{(M-1)} \end{bmatrix}_{\mathrm{current}} \right), \tag{26}$$

where $K \approx 4$–5, $L \approx 4$–5, $M \approx 4$–5, and $N \approx 4$–5 reflect effective neural/biomechanical bandwidth for spatial pose, printing cadence, viewpoint trajectory, and orbital parameter control,

respectively. The driver F_{drive} computes the next-order derivatives $g_{\mathcal{A}}^{(K)}$, $\omega_{\text{orb}}^{(N)}$, $r_{\text{orb}}^{(N)}$, $\Pi^{(L)}$, and $\Xi^{(M)}$ via jet-level pose steering, orbital frequency/radius modulation, intra-cycle cadence control, and SE(3) camera routing, all gated by the composite mapping jet J_Φ and hazard $h(t)$. H_{inertia} penalizes deviation from the current coupled configuration. Weights α and γ balance novelty-driven reconfiguration against habitual stability.

5 Access and printing modes

Let $\theta \in [0,\, 2\pi + \varepsilon)$ parameterize a local card/perimeter $\mathcal{A}$, where $\varepsilon > 0$ denotes a transient overshoot characteristic of compressed phasic motion. Define the *active-phase set* $\Pi(t) \subseteq [0, 2\pi)$:

$$\textbf{Phasic:} \quad \Pi(t) = \{\theta^*(t)\},\ \dot{\theta}^* = \omega_\theta, \tag{27}$$

$$\textbf{Compressed phasic:} \quad \Pi(t) = \{\theta^*(t)\} \text{ for } t \in [t_k, t_k + \tau_\theta],\ \varnothing \text{ otherwise}, \tag{28}$$

$$\textbf{Interrupt:} \quad \Pi(t) = \{\theta \,|\, \theta \in [0, 2\pi)\} \text{ at } t = t_k,\ \varnothing \text{ otherwise}, \tag{29}$$

$$\textbf{Extrusion:} \quad \Pi(t) = \{\theta \,|\, \theta \in [0, 2\pi)\}\ \forall t \in [t_0, t_1]. \tag{30}$$

These modes appear at any scale (micro/local vs. macro/global) and can nest, e.g., a smooth global carrier with local interrupt "cards." "Rolodex" arises from tidally-locked orbital or rotational macrocycles hosting interrupt microcards (another name for ringframes ρ).

6 Hazard-gated timing

Interrupt scheduling follows a point-process hazard

$$\boxed{h(t) = \beta(t) + \sum_i g(\alpha_i)\, k(t - t_i) - a(t),} \tag{31}$$

with baseline $\beta(t)$, mic events at times t_i with salience α_i, event kernel $k(\cdot)$, and adaptation $a(t)$. Likelihood and survival follow standard point-process form; Ogata thinning simulates exactly. Photic entrainment elevates visual hazards selectively; non-visual channels can run in parallel. In phasic regimes, $\beta(t)$ and $\mathcal{M}$ modulate trajectory rather than gate.

7 Semiosis cascade

RBT recasts Peircean semiosis as a three-stage temporal cascade:

1. **Perceptual:** mic/baseline (representamina) → prints ρ on $\mathcal{A}$ (interpretant) → proto-object.
2. **Cognitive:** proto-object drives $\mathcal{R}/\mathcal{I}$ reconstruction (interpretant), yielding object-level content.
3. **Metacognitive/action:** $\mathcal{R}/\mathcal{I}$ becomes representamen for threat/affordance interpretation, shaping behavior (object) [6].

8 Neural correlates and predictions

Hyperpolarization bottleneck. Dissociative states exhibit slow ($\sim$ 2 Hz) envelopes with fast bursts ($\sim$ 80 Hz) [3, 8]. RBT predicts interrupt-dominant access with long gaps, global cards per slow crest, and gamma bursts as print signatures.
Motor/temporal rings. Latent rotational trajectories in motor cortex and timing tasks map onto ringframes and card cadence [4, 5].

Photic entrainment. 10–13 Hz strobe locks visual-plane access; content planes may show multiple faster passes per attentional bin.
Cardiac-phase gating. Heartbeat-coupled mic events bias hazard $h(t)$, altering interrupt likelihood.
Vestibular "throw." Transients shift pose via Sim(3) perturbations, briefly re-siting $\mathcal{A}$ for re-lock.

Empirical program: EEG beta/gamma power crests synchronized with musical transients [7].

9 Methods sketch for testing

1. **Point-process modeling of frame events:** infer $h(t)$ from discrete "card" times (blink-aligned, saccade-aligned, photic-locked), compare baseline-only vs. +mic vs. +adaptation models.

2. **Dual-plane refresh:** separate an attentional plane (slow) from a content plane (fast) via cross-frequency nested rate analysis.

10 Phenomenology snapshots

Abortive wave. A global interrupt upon eye closure: $h(t)$ spikes, $\mathcal{A}$ prints against a black input, $\mathcal{R}$ fails to assemble rich paint; a turbulent ripple passes over the visual field plane.
Overexposure wave. Sudden bright entry causes a saturated print; the visual plane momentarily destabilizes under extreme luminance before re-stabilizing.
Gross→fine. A half-second chirp from $\sim 4 \to 40$ Hz prints successive geometric refinements (low to high geometric frequency; e.g., spatial frequency in 3D); color/paint arrives late [10].
Dissociation. Strong slow baseline with a transient, seconds-long anticorrelation of phase of brain regions may correlate with "true" dissociation (metacognition detaches from control of avatar in $\mathcal{R}$ and becomes observer-only).

11 Acknowledgments of prior observations

Carl Sagan's "Mr. X" imagery suggested outlines-first semiosis: "outlines of...instant appreciation" seems to describe $\mathcal{R}$ magically appearing from the operation of Π on $\mathcal{A}$ [6]. Lehar described cyclic gross→fine rendering and concentric scaffolds [9, 10]; see also Cube Flipper's exegesis [11]. Our prior EEG results showed beta/gamma power aligned to musical transients consistent with access gating [7].

12 Conclusion

RBT frames conscious semiosis as the geometry and timing of access followed by conceptual understanding. The Bank $\mathcal{B}$ (posed by Sim(3)), the Access Manifold $\mathcal{A}$, and the printing operator Π, together deliver ringframes ρ into the Time Schema $\mathcal{T}$ (guided by $\vec{C}$, driven by $\mathcal{M}(t)$ and $\beta(t)$), from which $\mathcal{R}$ and $\mathcal{I}$ are read out with latency. Baseline dynamics establish cadence; aboutness modulation steers pose/walk/timing to bind "what matters now." The hazard formalism unifies phasic modulation and interrupt gating, connecting phenomenology to testable neural signatures across normal, entrained, hyperpolarized (sedated), and anesthetized states. Hyperpolarization is thought to collapse distributed bank usage into a single embodied stream of phenomenology: as membrane potentials drift downward and NMDA-dependent excitation weakens, beta/gamma activity vanishes, and cortical dynamics become globally entrained—first around the alpha range

(∼10 Hz), then slowing into delta during deep sedation (2–4 Hz), and finally into ultra-slow oscillations near 1 Hz under anesthesia, where multiplexed access effectively ceases.

The hierarchical mapping architecture (§4.8) reveals that all schema poses reduce to the first-level mapping $\Phi_{\mathcal{R}_A \to \mathcal{A}}$ and its derivatives, while pose-jet control (§4.3) extends modulation from instantaneous pose to the full kinematic texture of velocity, acceleration, and snap. Orbital parameter jets (§4.4) further allow the Bank's orbit itself to evolve under aboutness control. Together, these structures make precise how conscious dynamics can feel simultaneously stable and fluid—inertial enough to maintain coherent orbits, yet responsive enough to redirect them within a single cycle.

Symbol/notation glossary

- $\mathcal{B}$: Bank (shape manifold), $S \in \mathcal{S}$ modulo translation/rotation/scale.
- Sim(3): similarity group (scale $s > 0$, $R \in \mathrm{SO}(3)$, translation $t \in \mathbb{R}^3$).
- $\mathfrak{sim}(3)$: Lie algebra of Sim(3); 7D vector space of body-frame velocities, accelerations, and higher derivatives pulled back from $T\,\mathrm{Sim}(3)$.
- $\exp : \mathfrak{sim}(3) \to \mathrm{Sim}(3)$: Lie group exponential, reconstructing pose from algebra-valued motion generators.
- $g(t) \in \mathrm{Sim}(3)$: pose/scale action placing S for display.
- $\mathcal{A}(t) \subset X_{\text{display}}(t)$: Access Manifold (local 0–2D).
- $\rho(t) = \Pi(\mathcal{A}, S, g)$: ringframe printed into $\mathcal{T}$.
- $\mathcal{T}$: Time Schema (fading buffer/flowfield).
- $\mathcal{R}, \mathcal{I}$: Real/Imaginal readouts reconstructed from recent ρ and context.
- $h(t)$: hazard (instantaneous print likelihood); $\beta(t)$: baseline cadence; $a(t)$: adaptation.
- $J_g^{(K)}(t)$: pose jet—temporal derivatives of $g(t)$ up to order K.
- $J_{\text{orb}}^{(N)}(t)$: orbital parameter jet—temporal derivatives of $\omega_{\text{orb}}, r_{\text{orb}}$, etc. up to order N.
- $\Phi_{\mathcal{R}_A \to \mathcal{A}}$: primary mapping from Real Schema Avatar to Access Manifold.
- $\Phi_{\mathcal{A} \to \mathcal{B}}, \Phi_{\mathcal{A} \to \mathcal{R}}, \Phi_{\mathcal{A} \to \mathcal{I}}$: secondary mappings slaved to $\mathcal{A}$.
- $\vec{C}(t)$: aboutness vector in concept space.
- $\mathcal{M}(t)$: mic signal (high-level structured drive).
- $\Xi_{\text{Cyclopean}}, \Xi_{\text{Mind's Eye}}$: observer cameras in SE(3).

References

[1] Caldwell, Brad (2022). *Rings of Fire: How the Brain Makes Consciousness.*

[2] Caldwell, Brad (2023). *Perceptual Optics.*

[3] Vesuna, S. et al. (2020). Deep posteromedial cortical rhythm in dissociation. *Nature.*

[4] Saxena, S., Russo, A. A., Cunningham, J., & Churchland, M. M. (2022). Motor cortex activity across movement speeds is predicted by network-level strategies for generating muscle activity. *Neuron*, 110(5), 839–855.

[5] Gámez, J., Mendoza, G., Prado, L., Betancourt, A., & Merchant, H. (2019). The amplitude in periodic neural state trajectories underlies the tempo of rhythmic tapping. *PLOS Biology*, 17(5), e3000054.

[6] Sagan, Carl. (n.d.). *Mr. X*. Organism Earth. Retrieved from `https://www.organism.earth/library/document/mr-x`.

[7] Caldwell, Brad. (2025). *Spectral Amplitude Modulation in EEG: Potential Correlations with Musical Stimuli*. Figshare. DOI: 10.6084/m9.figshare.27115354. `https://nodes.desci.com/dpid/419/v1`.

[8] Adam, E., Kowalski, M., Akeju, O., Miller, E. K., Brown, E. N., McCarthy, M. M., & Kopell, N. (2024). Ketamine can produce oscillatory dynamics by engaging mechanisms dependent on the kinetics of NMDA receptors. *PNAS*, 121(22), e2402732121.

[9] Lehar, Steven. (2008). *The Constructive Aspect of Visual Perception*.

[10] Lehar, Steven. (2010). *The Grand Illusion: A Psychonautical Odyssey*.

[11] Cube Flipper. (2022, November 22). *An introduction to Steven Lehar, part II*.

[12] Chang, S., Zhang, X., Cao, Y., Pearson, J., & Meng, M. (2025). *Imageless imagery in aphantasia revealed by early visual cortex decoding*. Current Biology, 35, 591–599. `https://firebasestorage.googleapis.com/v0/b/theoriesofconsciousness.appspot.com/o/Meng_2025.pdf?alt=media&token=8fedc858-c582-47de-8f9e-c2ed8039764a`

[13] Ronnie_Yonk. *[3D Model of Cobain and Stage]*. Cults. Retrieved [2022].

[14] GIGI_TOYS. *[3D Model of Driver/Wheel]*. Cults. Retrieved [2022].

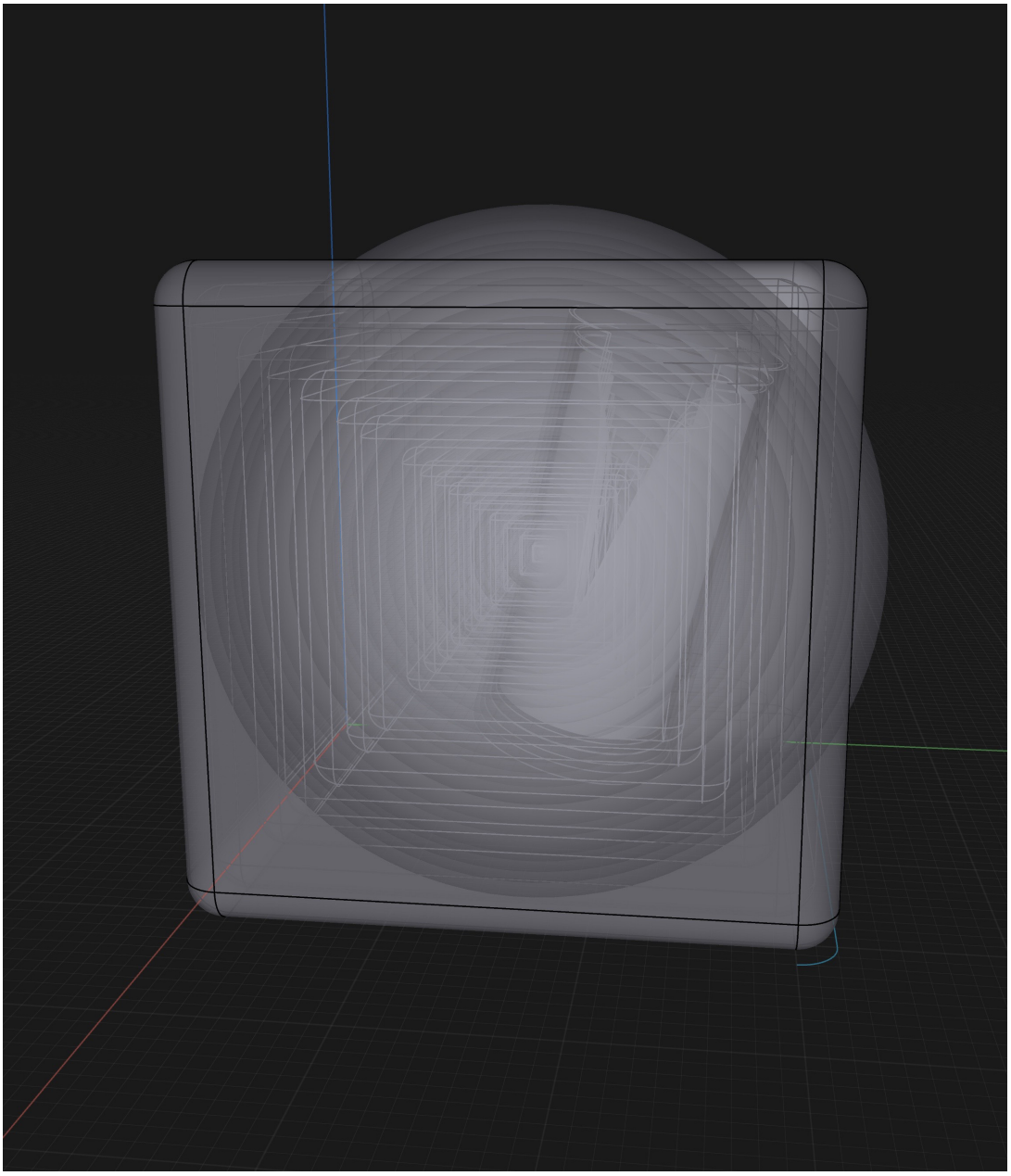

Figure 1: **Bank $\mathcal{B}$:** a shape in Kendall space posed by $g(t) \in \mathrm{Sim}(3)$ (scale, rotation, translation).

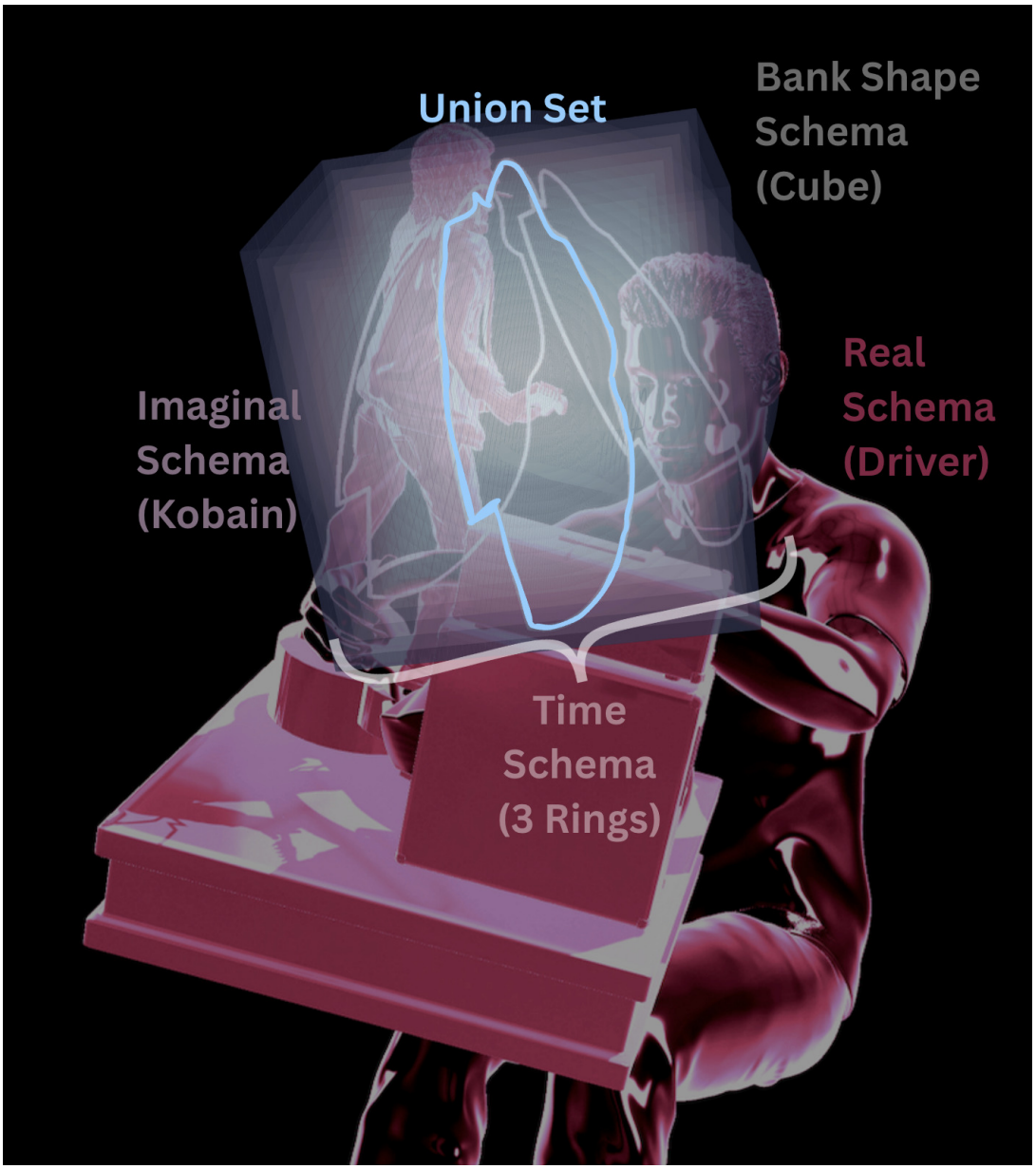

Figure 2: **Operational intersection vs. structural union:** multiple 3D schemas form $\mathcal{U}_{\text{struct}}$; conscious sampling occurs on the 0–2D access manifold $\mathcal{A}(t)$ ($\mathcal{A}$ is here labeled "union set," as in the shared, intersecting voxels between all schemas) (models from [13, 14]).

(a) Clear hemishell with frame triad (gaze, up, left)

(b) Painted hemishell with colored ray-rods

Figure 3: Incoming light is modeled as straight rays converging at the pupil. (a) A viewing-frame triad within a clear hemispherical dome. (b) A painted hemishell on $\mathbb{S}^2$ illustrates directions ω for $L_{\text{phys}}(\omega, \nu)$ and $L_{\text{perc}}(\omega)$. Real and mind's eye cameras $[\Xi_{\text{Cyclopean}}, \Xi_{\text{Mind's Eye}}]$ have SE(3) freedom within posed $\mathcal{R}$ and $\mathcal{I}$.

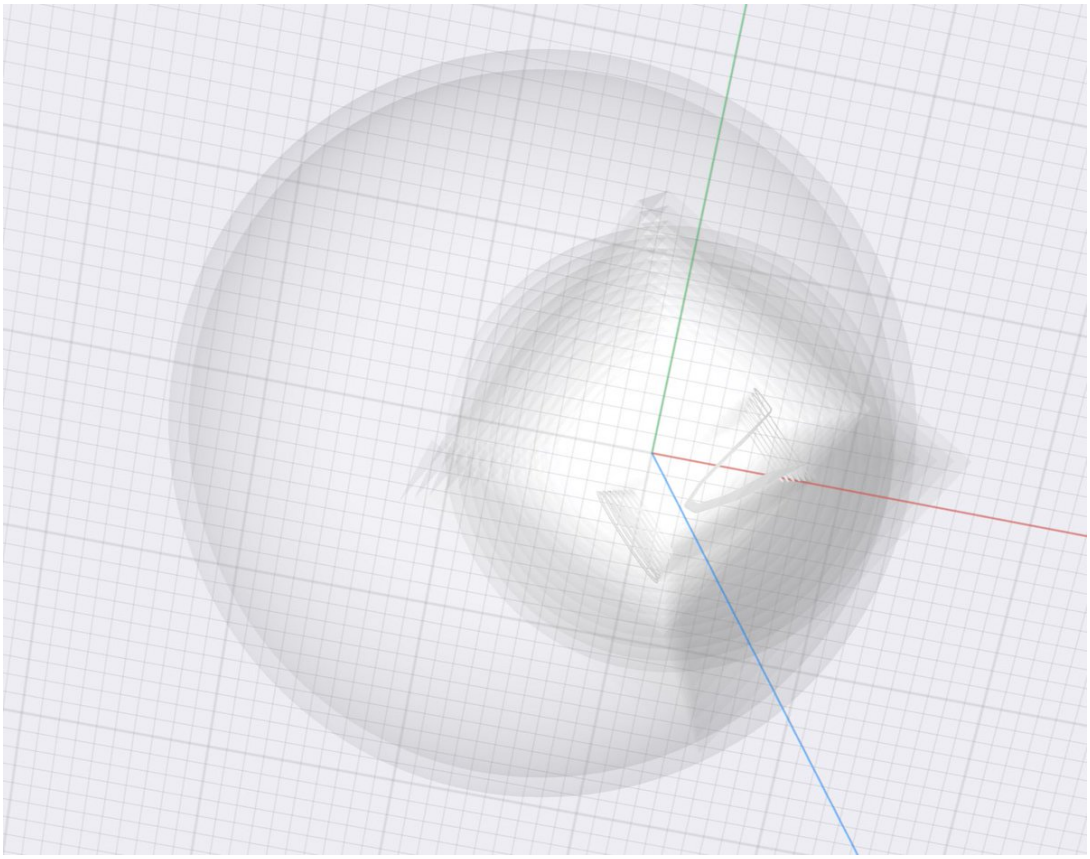

Figure 4: **Global "all-hot" spirographic mode:** the entire bank shell is active and moves as a unit under $g(t)$.

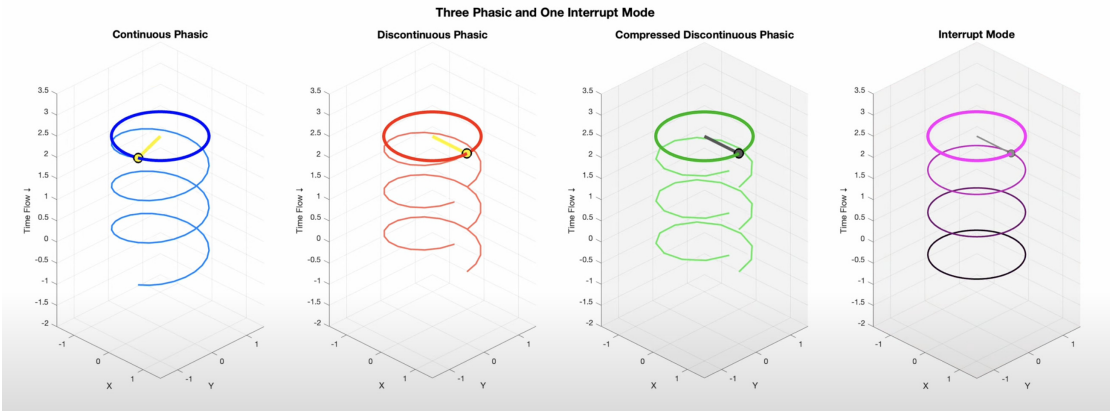

Figure 5: **Continuum of access:** phasic → compressed phasic → interrupt.

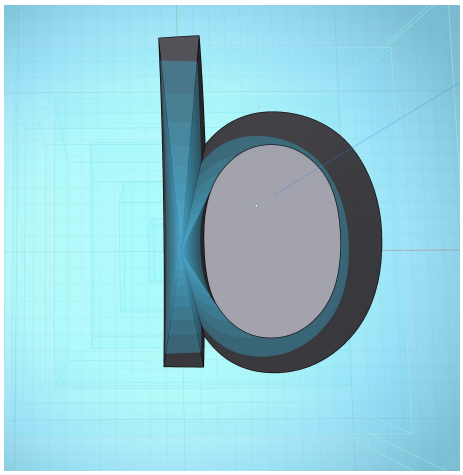

(a) Radial history gradient view

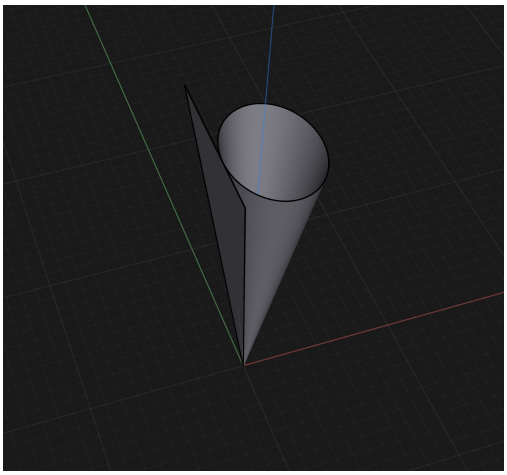

(b) Pure skewer geometry

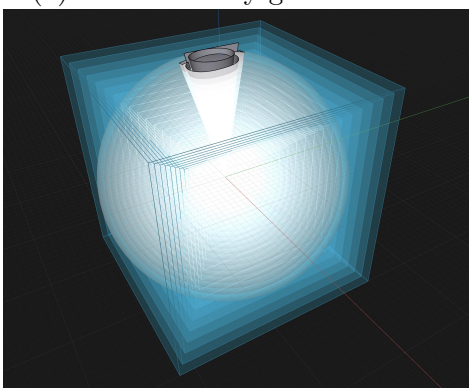

(c) Cross-section through bank

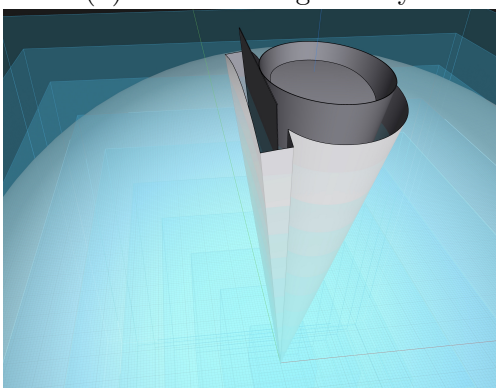

(d) Letter "b" skewer pathway

Figure 6: **Radial History Stack (Bank Skewer $\mathcal{B}_{\text{Sk}}$):** Content instances organize radially: present (outer) to past (inner). (a) Temporal gradient view; (b) Pure skewer geometry; (c) Cross-section through bank; (d) Letter "b" pathway. Enables overview of concept history when $\mathcal{A}$ prints nearby, supporting serial dependence and emotional pathway following. Skewer itself inferred; chasm/layers phenomenologically accessible but typically subconscious due to rapid printing, $\mathcal{R}$ dominance, and latch-on to most recent case.

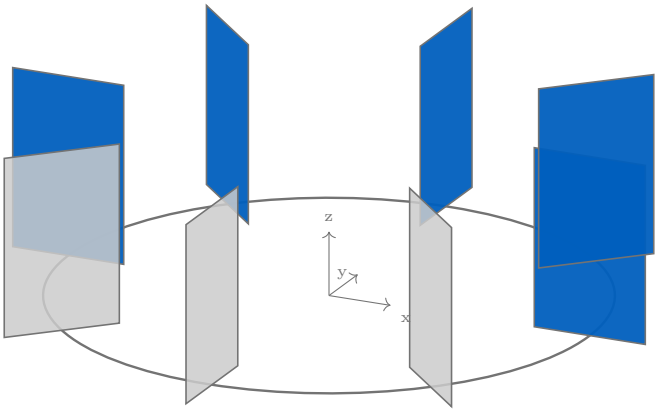

Figure 7: **Horizontal torus: 3D macrocycle with tangent-facing microcycle "cards."** Pattern: M=8, B=5 bright and 3 dark.

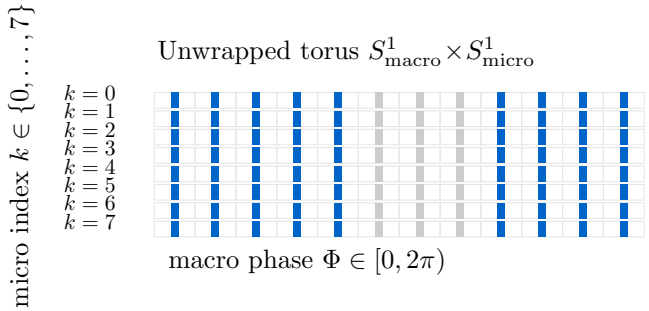

Figure 8: **Macro×micro torus (unwrapped, blip rendering).** One macrocycle (T_{macro}) with M=8 micro slots; pattern B=5 bright, 3 dark. Each slot shows a brief blip (bright or dim) with silence for the rest of the slot—matching interrupt-like micro-prints or compressed-phasic micro sweeps whose active fraction $d = \tau/T$ is small and hazard/adaptation-modulated.

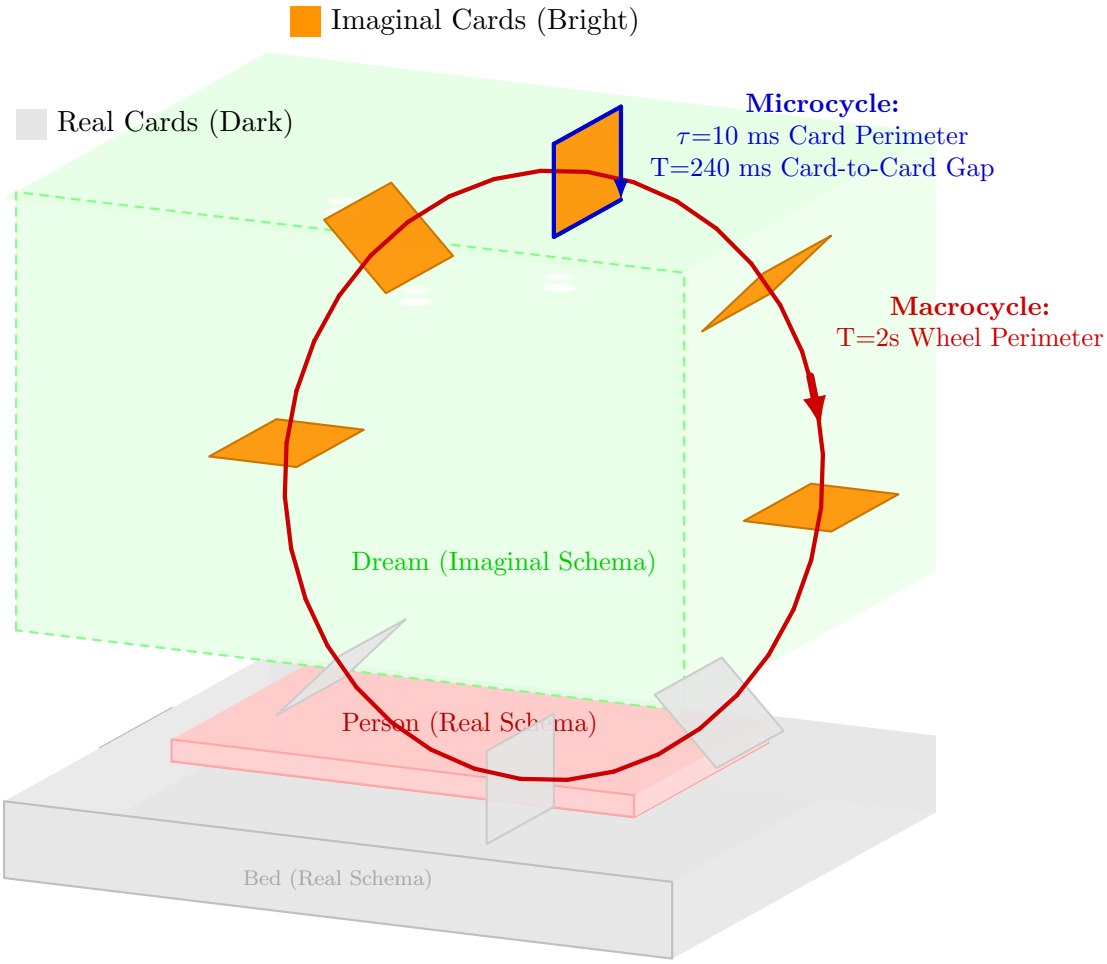

Figure 9: **Vertical (sagittal) torus ("paddlewheel"):** In this mode, the access manifold is a card-like plane (or its perimeter) carried around a 2-s macrocycle. It turns *hot* only in brief blips, spaced ∼250 ms apart (4 Hz), a pattern typical of hypnagogia as beta/gamma power wanes and global theta–delta entrainment rises. Each theta/delta crest corresponds to printing one card: upper-sector (bright) cards broadcast imaginal content; lower-sector (dim) cards lightly interface with the Real schema as the mic line shuts down and the baseline rhythm sets the dream frame rate. Timing: per-card perimeter microcycle $\tau_{\text{micro}} \approx 10$ ms (near-instant sweep), inter-card period $T_{\text{micro}} \approx 250$ ms, macrocycle $T_{\text{macro}} \approx 2$ s.

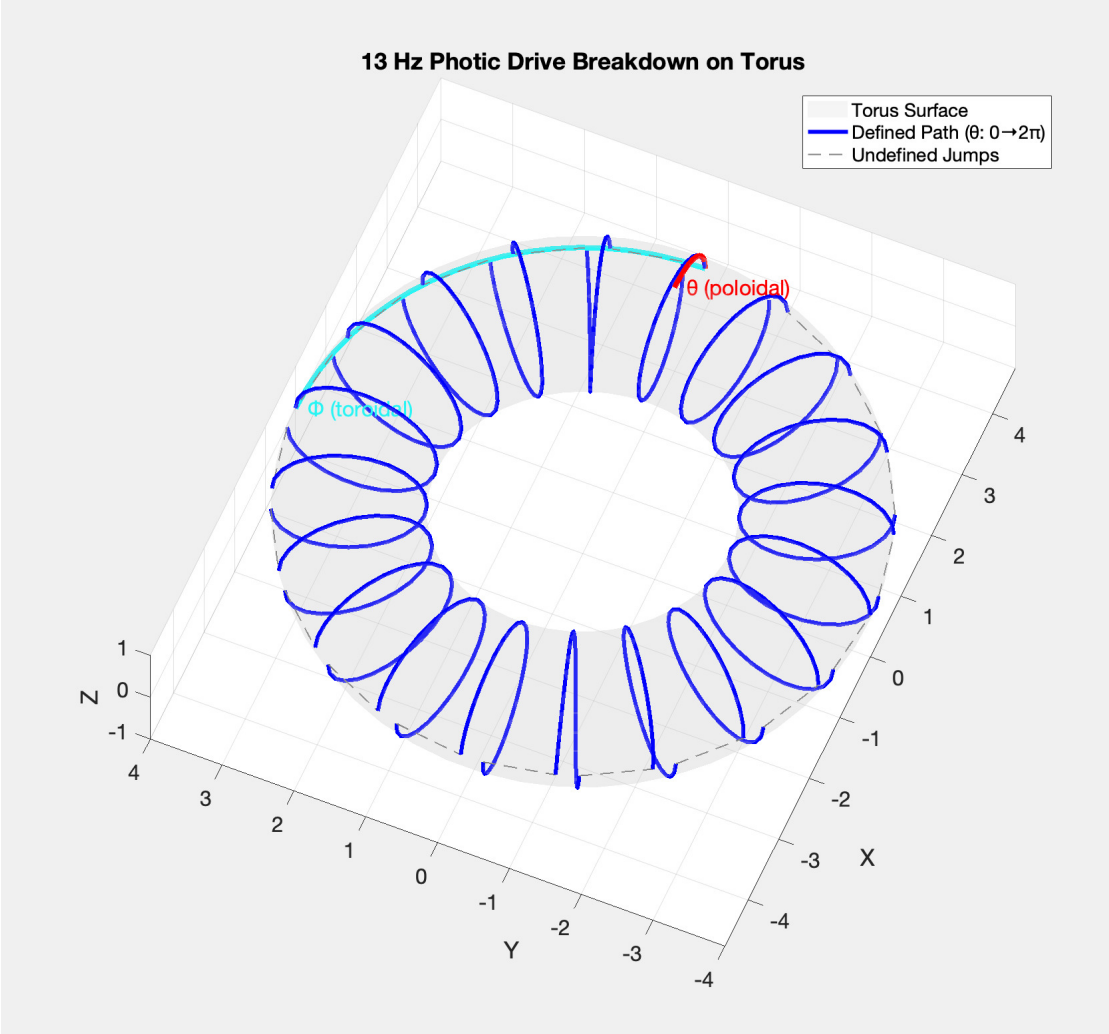

Figure 10: **Photic Drive Breakdown:** Under 13 Hz strobe entrainment, $\mathcal{B}$ (and thus $\mathcal{A}$) rotate in a tidally locked orbit. In light hyperpolarization, the "paint" flash may fragment into $\mathcal{B}$ revolving 13 times per second, printing one bright flash-card per revolution and leaving a trace of higher-frequency ($\sim$260 Hz) dark cards. Roughly 20 cards are produced per revolution, implying spatial–temporal precision of $\sim$200 μs in modeling space.

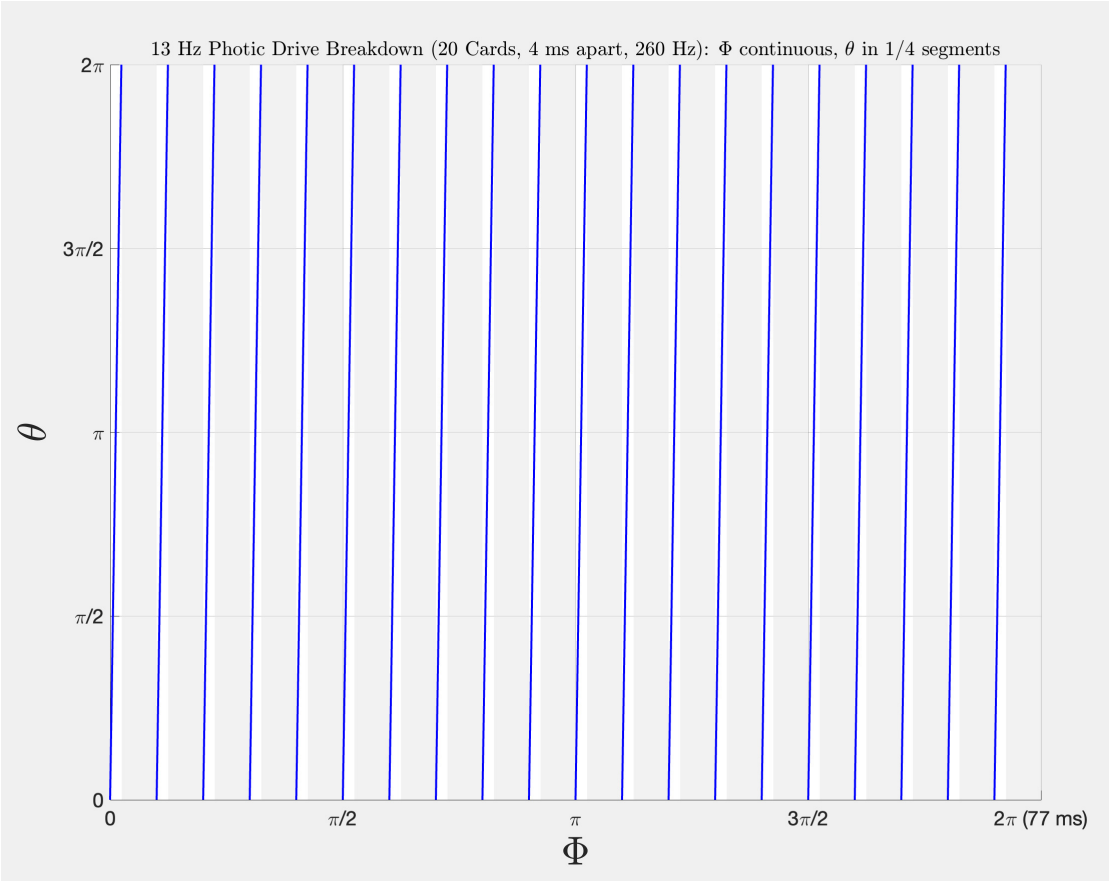

Figure 11: **Unwrapped Breakdown:** As $\tau \to 0$, each card's local θ-phase compresses into a near-instant blip, leaving most of the card-to-card microperiod T silent or passive.

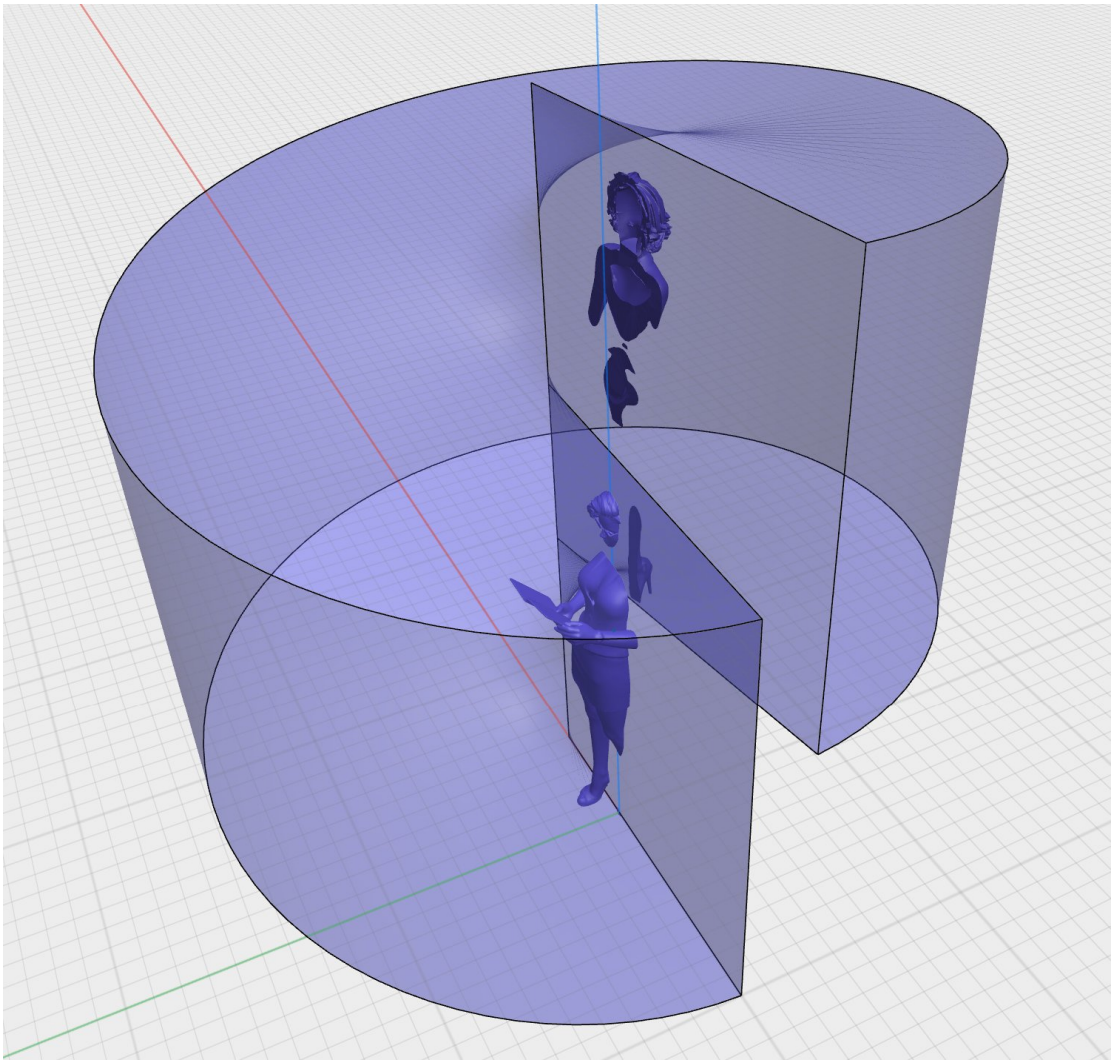

Figure 12: **Global mode example (shown as compressed phasic):** A macrocycle contains a compressed active phase τ within a larger period T (major circle of the torus). A hot plane—locally in **extrusion mode**—completes one revolution during τ, then holds its pose for the remainder of T ($\tau < T$).

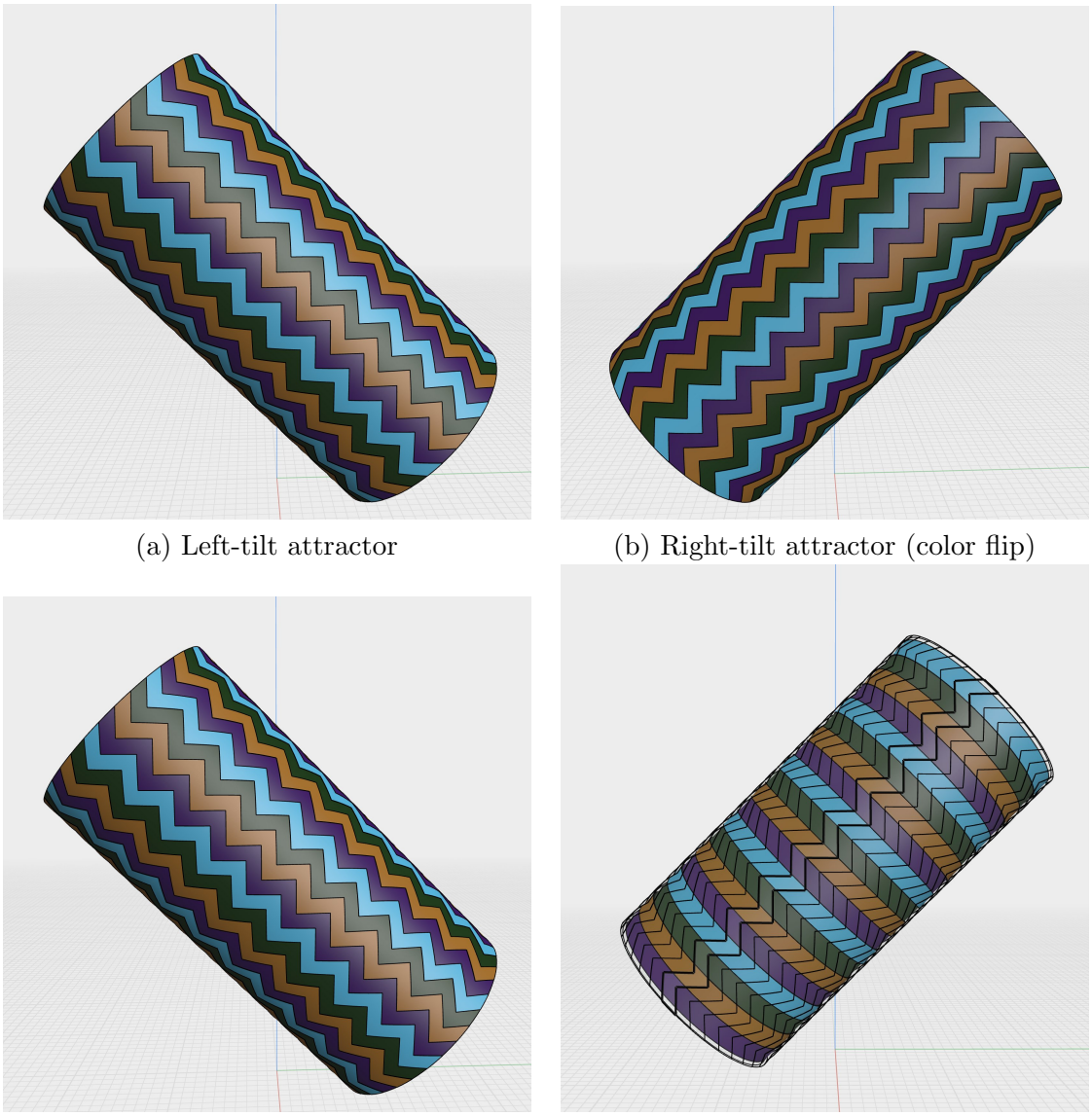

(a) Left-tilt attractor

(b) Right-tilt attractor (color flip)

(c) Left-tilt attractor

(d) Right-tilt attractor (no color flip)

Figure 13: **Photic-entrainment zigzag attractors:** During photic drive, one sees flashing, which may break down into hallucinatory attractors such as grids, chessboards, square tunnels, etc., and there may be epochs (roughly 5–60 seconds long) where the Bank cylinder displays parallel chevron patterns that are bistable, succumbing to a left-tilt configuration for $\sim$10 s before tiring and switching to a right-tilt configuration for $\sim$10 s. During a single stable configuration, the Bank's cylinder (depicted, not visible, only assumed)—along with the rest of the Bank (not depicted, not visible)—may follow an orbital path, laying the chevrons down into the wall of a larger cylindrical cavity, as if viewing from inside (this is visible). The cylinder's orbital path is thus akin to spirographic printing of a rotor within a stator. Orbit frequency varies in real time but typically ranges from 0.5 to 13 Hz. Top row shows a color-flip transition; bottom row shows a no-color-flip transition. The inter-line spacing between the two most-emphasized zigzag lines (one emphasized per cycle, alternating back-and-forth) typically shrinks while frequency increases as the system approaches attractor shift, which decreases the opacity and stability of the current attractor's visuals. The transition involves the entire interpretation rotating 90° to form an X-pattern if a 20-second exposure were used.